AD-A038 915 LOCKHEED MISSILES AND SPACE CO INC PALO ALTO CALIF PA--ETC F/6 10/3
DETECTION OF ELEMENTARY PROCESSES WITHIN POROUS ELECTRODES.(U)
APR 77 S SZPAK, T KATAN N00014-73-C-0397
UNCLASSIFIED LMSC-D558466 NL

| OF |
AD
A038915

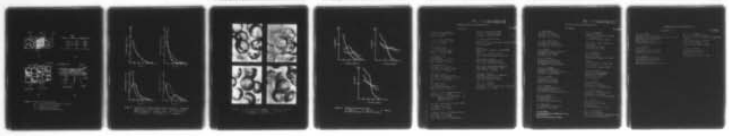

END

DATE
FILMED
5-77

OFFICE OF NAVAL RESEARCH
Contract N00014-73-C-0397
TECHNICAL REPORT NO. 5

DETECTION OF ELEMENTARY PROCESSES WITHIN POROUS ELECTRODES

by
S. Szpak and T. Katan

Prepared for Publication
in the
Journal of the Electrochemical Society

Lockheed Palo Alto Research Laboratory
Lockheed Missiles & Space Company, Incorporated
A Subsidiary of Lockheed Aircraft Corporation
Palo Alto, California 94304

April 18, 1977

(14) TR-5

MIL-STD-847A
31 January 1973

Unclassified
SECURITY CLASSIFICATION OF THIS PAGE (When Data Entered)

REPORT DOCUMENTATION PAGE		READ INSTRUCTIONS BEFORE COMPLETING FORM
1. REPORT NUMBER: Technical Report No. 5	2. GOVT ACCESSION NO.	3. RECIPIENT'S CATALOG NUMBER
4. TITLE (and Subtitle): Detection of Elementary Processes Within Porous Electrodes		5. TYPE OF REPORT & PERIOD COVERED: Interim rept.
		6. PERFORMING ORG. REPORT NUMBER: LMSC No. D558466
7. AUTHOR(s): S. Szpak, T. Katan		8. CONTRACT OR GRANT NUMBER(s): N00014-73-C-0397
9. PERFORMING ORGANIZATION NAME AND ADDRESS: Lockheed Palo Alto Research Laboratory, Materials Sciences, Palo Alto, Calif. 94304		10. PROGRAM ELEMENT, PROJECT, TASK AREA & WORK UNIT NUMBERS
11. CONTROLLING OFFICE NAME AND ADDRESS: Office of Naval Research, 800 North Quincy Street, Arlington, Virginia 22217		12. REPORT DATE: 18 April 1977 (12) 16p. 13. NUMBER OF PAGES: 14
14. MONITORING AGENCY NAME & ADDRESS (if different from Controlling Office)		15. SECURITY CLASS. (of this report): Unclassified 15a. DECLASSIFICATION/DOWNGRADING SCHEDULE

16. DISTRIBUTION STATEMENT (of this Report)

Approved for Public Release; Distribution Unlimited

17. DISTRIBUTION STATEMENT (of the abstract entered in Block 20, if different from Report)

18. SUPPLEMENTARY NOTES

Prepared for publication in the Journal of the Electrochemical Society

19. KEY WORDS (Continue on reverse side if necessary and identify by block number)

porous electrodes, electrode design, batteries, electrode modeling

20. ABSTRACT (Continue on reverse side if necessary and identify by block number)

The interaction of elementary processes within the confines of porous structures is simplified by application of concepts such as penetration depth and a structural unit characteristic of porous electrodes. A systematic approach to the determination of relevant processes and specification of electrode structure is presented. Both experimental and mathematical analogs are used.

DD FORM 1 JAN 73 1473 EDITION OF 1 NOV 65 IS OBSOLETE

Unclassified
SECURITY CLASSIFICATION OF THIS PAGE (When Data Entered)

210 118

DETECTION OF ELEMENTARY PROCESSES WITHIN POROUS ELECTRODES

S. Szpak, T. Katan
Naval Ocean Systems Center, San Diego, CA 92152
Lockheed Missiles & Space Co., Inc.
Lockheed Palo Alto Research Lab, Palo Alto, CA 94304

ABSTRACT

Problems in electrode modeling are reduced if participating processes are recognized and experimentally defined. Difficulties in treating complex interplay between elementary processes within confines of a changing porous structure are minimized through application of simple concepts, *e.g.*, penetration depth and a structural unit characteristic of a porous electrode. A systematic approach to the determination of relevant processes and to specification of electrode structure for a prescribed performance is examined. The analysis is applied to the Ag/AgCℓ system in 1 N KCℓ operating at 23°C.

In work concerned with electrodes for electrochemical systems, particularly in the field of energy conversion and storage, two decisive design factors have emerged: reaction intensity profile and thickness of the porous electrode. This generalization applies equally to fuel cells, to various hybrid systems as well as to conventional batteries. This seems to imply that a rational electrode design should proceed via an electrode modeling approach.

The mathematics of electrode modeling has advanced to a high degree of sophistication. Today's models, chiefly due to efforts of Bennion and Newman and their co-workers(1), are applicable to complex situations. These models are capable of handling such factors as changes in surface morphology, reaction kinetics and the transport properties. These factors however, must be determined experimentally so that correct computer inputs can be provided for the various systems under consideration. The present status may be summarized as follows: the mathematics of electrode modeling are well developed but the realistic, experimental, inputs required for meaningful modeling are lagging behind.

It is the purpose of this communication to examine methods by which elementary processes operating within the porous structure can be detected and identified. The emphasis is on the use of a concept of penetration depth and the examination of surface morphology. The analysis is applied to the Ag/AgCℓ system in 1 N KCℓ operating at room temperature.

ELECTRODE ANALOGS AND SIMULATION OF OPERATION

Studies of the dynamics of porous electrode operation suggest that structural analogs can be constructed to provide useful tools in guiding the development of practical battery electrodes.(2,3) To illustrate, consider Fig. 1 where a set of elementary processes usually associated with an electrochemical reaction, Fig. 1b, are taking place within the confinements of a pore, Fig. 1a. If we accept the premise that the characteristics of a porous electrode can be represented by a set of events on planar electrodes which operate subject to local constraints on the reaction path, then the search for correct inputs for the electrode modeling may be accelerated.

Consider Fig. 2 to relate the experimentally simulated reaction intensity profile to that associated with the operation of a real porous electrode. In particular, Fig. 2a represents a real electrode structure. For the purpose of construction of an analog, we select a volume element sufficiently large compared to the individual grains, but small enough compared to the penetration depth. The electric circuit analog is shown in Fig. 2b while the experimental arrangements, or the structural analogs, are shown in Figs. 2c and 2d. Specifically, Fig. 2c shows a small section of an electrode structure generated by a loose packing of metallic spheres while Fig. 2d illustrates the principle and construction of a segmented electrode.

The concept of an electric circuit analog is introduced here to provide a basis for an elementary treatment of porous electrodes. Thus, it is assumed that in real porous electrodes, the position dependent current $i(x)$ and potential $u(x)$ in the electrolyte phase are related by Eqs. (1) and (2)

$$\frac{\partial u}{\partial x} + Ri = 0 \tag{1}$$

$$\frac{\partial i}{\partial x} + \frac{u}{Z} = 0 \tag{2}$$

The solution of Eqs. (1) and (2) exhibits an exponential behavior with a curvature which is dependent on the numerical value of $\kappa^2 = R/Z$. For a sufficiently thick electrode, the solution is

$$y(x) = A \exp(-\kappa x) \tag{3}$$

where $y(x)$ stands for either $i(x)$ or $u(x)$ and A is determined from the applicable boundary condition. However, because $j = -\partial i/\partial x$ and, for a conductive matrix, $u(x) = \eta(x) + \text{const.}$, it follows that $y(x)$ yields the reaction intensity profile, $j(x)$, as well as the distribution of the driving force, the overpotential, $\eta(x)$.

The characteristic number, κ, governing the distribution functions within the porous structure has been converted to a useful engineering

number. It has been used in the design of chemical reactors since 1939 and was defined simply as the ratio of transport resistance to the reaction impedance.(4) It was in this form that Bro and Kang(5) applied it to describe the behavior of sintered cadmium electrode. In electrochemical engineering its significance was clearly expressed by Wagner(6) and it gained acceptance in the 1960's in connection with the design of fuel cell electrodes.

A selected set of the characteristic number, together with respective author's formulation and nomenclature, are presented in Table I.

TABLE I.

Selected Examples of Formulation of the Characteristic Number

Author	Formulation	Nomenclature
Bro and Kang (5)	$\frac{\text{ionic impedance}}{\text{faradaic impedance}} = B^2$	electrochemical Thiele modulus
Wagner (6)	$k_c = \frac{\sigma RT}{\alpha_c zFJ}$	polarization parameters
Nanis (7)	$N^2 = \left[\frac{1}{L}\frac{\partial n}{\partial j}\right] \cdot \frac{1}{L(S/V)}$	throwing power
Grens and Tobias (8)	$\xi = \frac{a\,\ell^2\,i_o}{nFD_k C_k^{\,o}}$	transfer current distribution parameter
Gidespow and Baker (9)	$\phi^2 = \frac{i_o\,nF\,aL^2}{RT\,\kappa}$	dimensionless exchange current
Alkire and Mirarefi (10)	$\xi = \frac{2nF\ell^2\,i_o}{R_g T\,R_o \kappa}$	dimensionless reaction velocity parameter
Winsel (11)	$\lambda^2 = \frac{a\,RT}{2\rho F j_o}$	effective depth of penetration

Physical meaning of the characteristic number. The characteristic number can be formulated either as a dimensionless number, in a form indicating the curvature of the distribution function, or as a measure of penetration of the reaction zone into the electrode

structure. It also can be viewed as a product of quantities associated with the electrode reaction, inclusive of transport and properties of electrode structure. This is apparent in Nanis'(7) formulation.

To illustrate the kinetic nature of the penetration depth and to relate it to the electrode structure, consider Fig. 2d and apply Eq. (1) to an element dx, in a form

$$ai(x) = -\sigma\, a\, du/dx \tag{4}$$

where a is the spacing between the electrode segment and the glass cover, and σ is the electrolyte conductivity. Eq. (4) together with an expression for charge conservation

$$d(ai)/dx + j = 0 \tag{5}$$

yields, upon substitution of Eq. (5) into Eq. (4), a differential equation

$$\frac{d}{dx}\left[\sigma a \frac{d\eta}{dx}\right] - j = 0 \tag{6}$$

Assuming for simplicity a constant a and σ, and linearizing the Tafel-like $j(\eta)$ relation, we obtain the familiar equation

$$\frac{d^2\eta}{dx^2} - \left[\frac{RT}{\sigma a F}\, j_o\right] \eta = 0 \tag{7}$$

and therefore also an expression for the characteristic length which can be written in the form of a product of the electrode reaction parameters and the geometry of segmented electrode, namely

$$L_f^2 = \left[\frac{F j_o}{RT}\ \sigma\right] \cdot a \tag{8}$$

It is easy to see, cf., Fig. 2d, that $a = V/S$, where V is the electrolyte volume and S the interphase area. For an arbitrary electrode structure, a is replaced by $\phi = \langle V\rangle/\langle S\rangle$, cf., Fig. 2c. The structural parameter, ϕ, will remain constant as long as the structural unit is maintained.(12)

The effect of a change in the reaction path on the electrode behavior can now be examined in terms of the characteristic length. To account for any additional step, the so-called approach step(13), we may write an expression

$$j = -j_o\left[\exp\left(-\frac{F\eta}{RT}\right) - 1\right] \Big/ \left[1 - j_o \exp\left(-\frac{F\eta}{RT}\right)/F\ell RT\right] \tag{9}$$

The less familiar symbol, ℓ, is the phenomenological coefficient which relates the reaction velocity, $\vec{v}$, to the driving force, $\tilde{A}$. To account for the set of contributing processes, we proceed as follows: the electrochemical affinity, $\tilde{A}$, of the overall process is taken to be equal to the sum of affinities of the individual elementary processes, i.e.,

$$A = \sum_k A_k \qquad (k = 1, 2, 3, \ldots.) \tag{10}$$

By Eq. (10), only a set of consecutive reactions is allowed. For a stationary state: $\vec{v}_1 = \vec{v}_2 = \ldots = \vec{v}_k = \vec{v}$, and because of the relationship $\vec{v}_k = \ell_k \tilde{A}_k$, we have immediately

$$\ell^{-1} = \sum_k \ell_k^{-1} \tag{11}$$

Substitution of Eq. (11) into Eq. (9), yields

$$j = -j_o \left[\exp\left(-\frac{Fn}{RT}\right) - 1 \right] \Big/ \left[1 - j_o \exp\left(-\frac{Fn}{RT}\right) \sum_k \ell_k^{-1} / FRT \right] \tag{12}$$

A linearization of Eq. (12) and its substitution into Eq. (7) results in an expression for the characteristic length

$$L^2 = L_f^2 - \frac{\Sigma_k \ell_k^{-1}}{F^2} \sigma \cdot a \tag{13}$$

and illustrates how contributions due to the set of consecutive reactions contract the penetration depth. This result is in agreement with Grens'(14) earlier calculations showing the effect of transport restrictions on the reaction intensity profile. Evidently, the shift in the reaction profile may arise from any contribution to the set.

APPLICATION TO Ag/AgCℓ SYSTEM

If the reaction path remains unchanged, the electrode behavior is well simulated using the simple concept of invariant profile. This is always true for small time intervals, for the steady state or for the early stages of battery operation. However, in the course of battery operation the reaction profile is not invariant either because of a continuous change in the reaction path or a change in the electrode structure. A description of this interaction requires the solution of a set of differential equations whose number depends upon the desired completeness of solution.

Penetration depth-comparison with experiment. In recent communications(2,3), we examined the evolution of reaction profile and found a good agreement between the observed behavior recorded for the simulated electrode and that obtained by a totally different method in a structure resembling actual electrodes. A question thus naturally arises as to the reasons for such agreement. In an attempt to answer this query, consider the following: characterization of a porous structure is a difficult task because distribution functions (the averages) cannot be determined unambiguously. That is, different distribution functions can be realized for the same porous material depending upon methods and properties selected for comparison. On a basis of rather general considerations, Newman(16) showed that only three averages appear in the treatment of porous electrodes. These averages, indicated in Figs. 2c and 2d, are: (a) an average involving the cross section, i.e., an average based on cutting through the matrix and electrolyte, <A>; (b) an average over the interfacial area, <S>; and (c) an average over the volume, <V>. Thus, similarity in electrode behavior may be anticipated for electrodes having the same averages.

In order to check this assertion and our basic premise concerning the relation between the events occurring on planar electrodes and the effect of restraints imposed by the porous structure, we have considered penetration depths experimentally determined for three vastly different structures and by three different methods and compared them with values calculated using the characteristic number. Results, given in Table II, show the anticipated agreement when suitable structural parameters are selected for systems at their early stages of operation.

TABLE II.

Calculated and Observed Penetration Depths for Various Electrode Structures in 1 N KCℓ at 23°C.

structure	structural parameters	penetration depth, cm observed	calculated
Segmented electrode	a = 60μm S = 0.077 cm^2	$(8 \pm 0.3)10^{-2}$	7×10^{-2}
Flotronics electrode (membrane)	ε = 0.57 S = 4720 cm^{-1}	$(0.6 \pm 0.02)10^{-2}$	0.55×10^{-2}
Sphere-bed electrode	ε = 0.373 S = 1010 cm^{-1}	$(1.0 \pm 0.2)10^{-2}$	0.95×10^{-2}

Identification methodology. In this section, we quote some of the earlier results(2,3,15) to demonstrate how the concept of the penetration depth can be used to determine the probable elementary processes taking place at the onset of the electrode charging and how they change on prolonged operation.

The evolution of reaction profile during the first minutes of the passage of an anodic current, $i(0,t) = 50$ mA cm^{-2}, through a packed spheres electrode analog, is shown in Fig. 3. The transfer current density distribution, $j(x,1)$, is given in Fig. 3a for one minute after the commencement of electrode operation, while Figs. 3b, 3c, and 3d display profiles attained as indicated, i.e., $j(x,2)$, $j(x,5.5)$, and $j(x,7.5)$, respectively. In addition, to accentuate the evolution of profiles for diagnostic purposes, we have shown also two successive distributions in Figs. 3b, 3c, and 3d.

In order to arrive at the probable set of events, consider the evolution of the current density profiles in terms of Eq. (13). Moreover, assume that no change in the electrode structure has occurred within the first two minutes, a reasonable assumption in view of Figs. 4a and 4b. It follows therefore that either the electrolyte conductivity has changed, i.e., $\sigma(x,1) > \sigma(x,2)$, or a change has occurred in the dominant step of the overall process, thus shifting the reaction zone accordingly (cf. dashed and solid lines in Fig. 3b). At a later time, e.g., after 5 minutes of electrode operation, we noted the development of a "hump" which moves deeper into the electrode structure reaching a halfway point at $t = 7.5$ minutes.

The examination of surface morphology in the frontal region within the penetration distance of ca 0.1 mm, Figs. 4c and 4d suggests that the formation of a "hump" is due to blockage of the second kind(3). As the electrode charging continues, the frontal region becomes heavily coated, Fig. 4d, which, together with the observed steep profile, Fig. 3d, indicates reaction control by the transport of reactant from the bulk electrolyte.

In an attempt to provide additional evidence, we plotted reaction profile at comparable times for a series of charging currents, namely for $i(0,t) = 200$, 300, and 400μA. The results, shown in Figs. 5a, 5b, and 5c, are in agreement with the above analysis. In addition, however, they point to the importance of blocking of the second kind for open structures and to the importance of blocking of the first kind(3) for the electrodes characterized by a large surface to volume ratio.

CONCLUDING REMARKS

The inaccessibility to direct observation usually associated with the investigation of porous electrodes can be substantially overcome by the use of structural analogs. The segmented electrode arrangement

appears to be a convenient tool for following the evolution of reaction profiles.

A characteristic number, the penetration depth, can be formulated as a product of kinetic and structural parameters. Such formulation is essential for the interpretation of the probable operating processes and for qualitative assessment. However, additional evidence, e.g., SEM examination of surface morphology is desirable to differentiate between alternatives.

The limitations of structural analogs as diagnostic tools are primarily due to size of individual segments and of spacing containing the electrolyte. These difficulties appear to be alleviated by employment of methods and procedures common to the microelectronic industry.

ACKNOWLEDGMENT

This work was supported in part by the Office of Naval Research.

REFERENCES

1. J. Newman and W. Tiedemann, AICHE Journal, 21, 25 (1975).

2. S. Szpak, A. Nedoluha and T. Katan, J. Electrochem. Soc., 122, 1054 (1975).

3. S. Szpak and T. Katan, J. Electrochem. Soc., 122, 1063 (1975).

4. E. W. Thiele, Ind. Eng. Chem., 31, 916 (1939).

5. P. Bro and H. Y. Kang, J. Electrochem. Soc., 118, 519 (1971).

6. C. Wagner, Plating, 48, 997 (1961).

7. L. Nanis, Plating, 58, 805 (1971).

8. E. A. Grens and C. W. Tobias, Ber. Bunsenges., 68, 236 (1964).

9. D. Gidaspow and B. S. Baker, J. Electrochem. Soc., 120, 1005 (1973).

10. R. Alkire and A. A. Mirarefi, J. Electrochem. Soc., 120. 1507 (1973).

11. A. Winsel, Z. Elektrochem., 66, 287 (1962).

12. T. Katan and H. F. Bauman, J. Electrochem. Soc., 122, 77 (1975).

13. P. Van Rysselberghe, in "Modern Aspects of Electrochemistry," Vol. 4, Plenum Press, New York, 1966.

14. E. A. Grens, Electrochim. Acta, 15, 1047 (1960).

15. T. Katan, S. Szpak and D. N. Bennion, J. Electrochem. Soc., 121, 757 (1974).

16. J. Newman, quoted by J. S. Dunning, Dissertation, UCLA 1971.

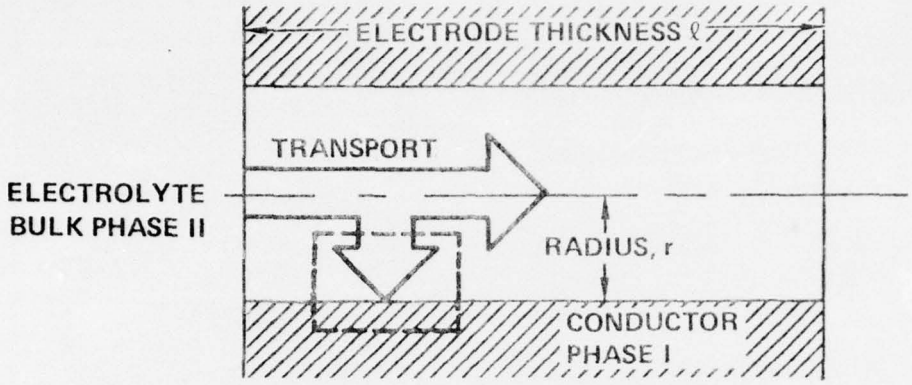

(a)

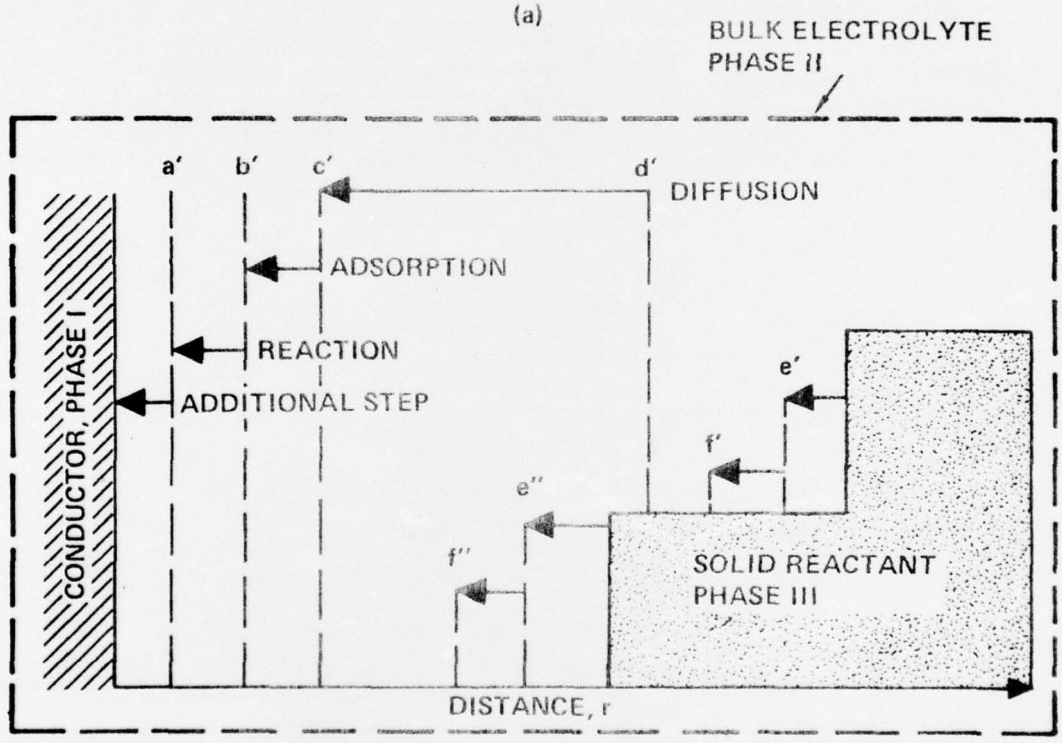

(b)

Figure 1. Elementary processes for the case: sparingly soluble reactant (phase III)-conductive matrix (phase 3), operating under dissolution-diffusion mode.
a. - single pore analog.
b. - set of consecutive elementary processes.

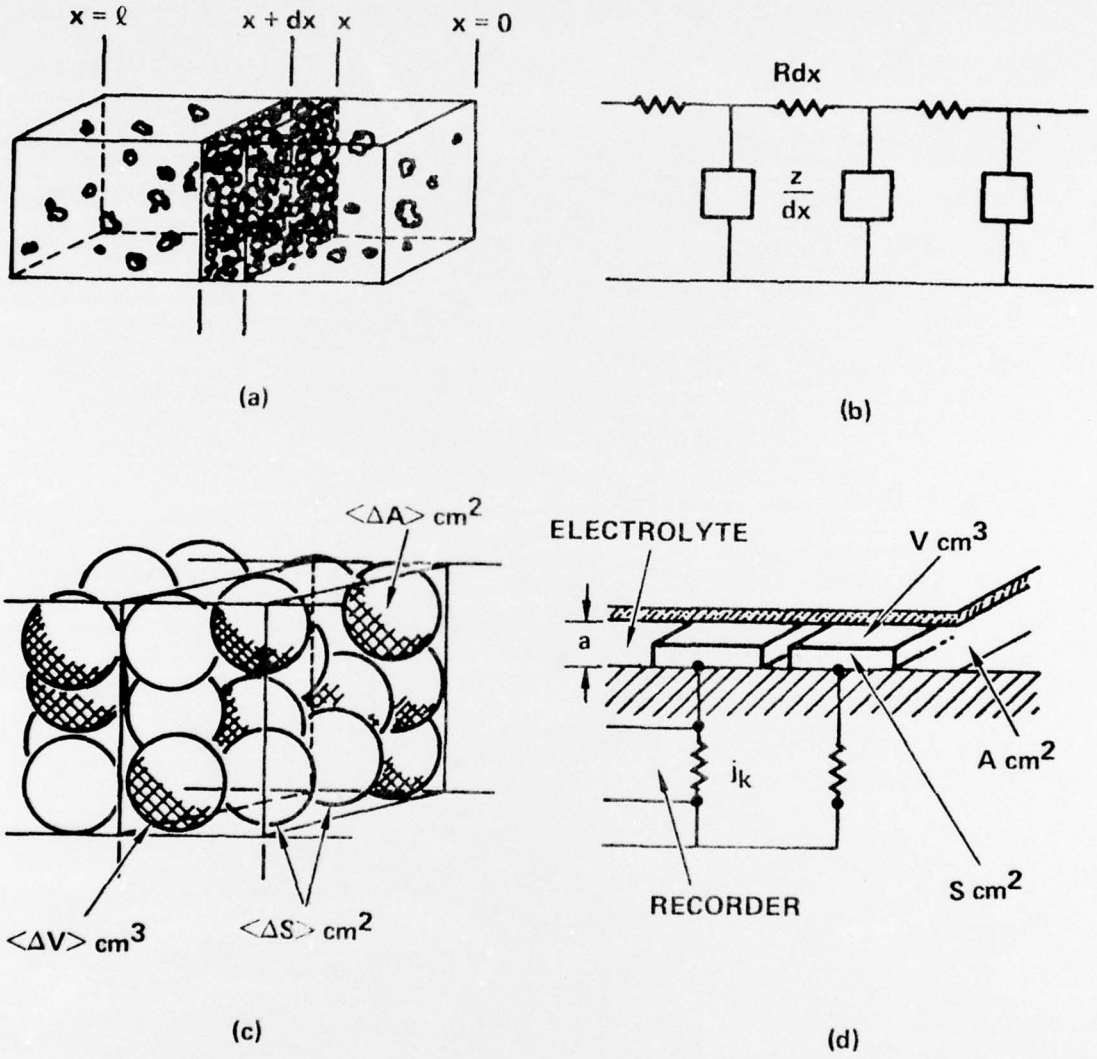

Figure 2. Porous structure analogs.
a. - real electrode structure (schematic).
b. - electric circuit analog.
c. - packed sphere analog.
d. - segmented electrode analog.

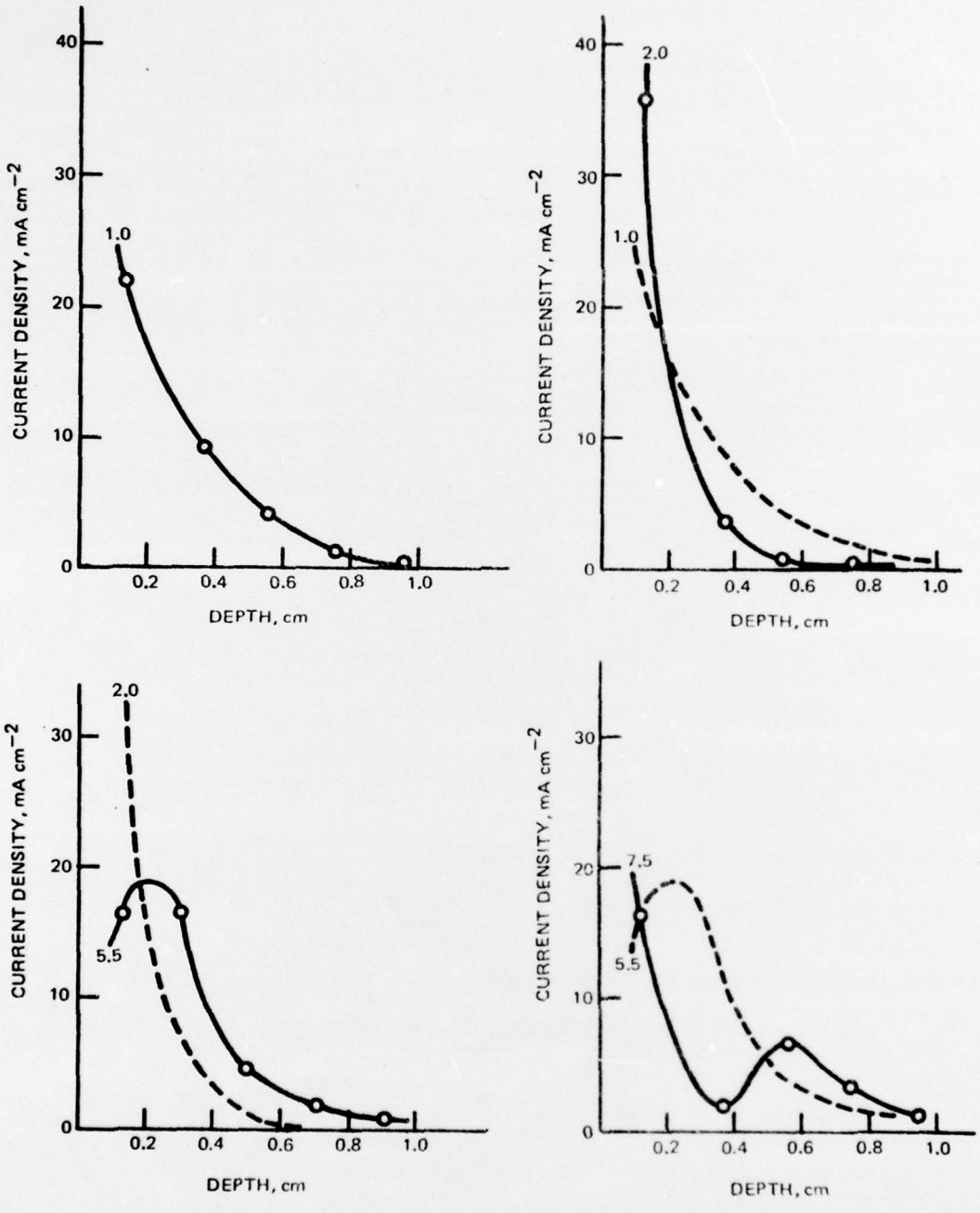

Figure 3. Evolution of transfer current density profiles. Structure-packed spheres; electrolyte 1 N KCℓ; superficial current density 50 mA cm^{-2}. Charging times: a - 1.0 minute, b - 2.0 minutes, c - 5.5 minutes, d - 7.5 minutes.

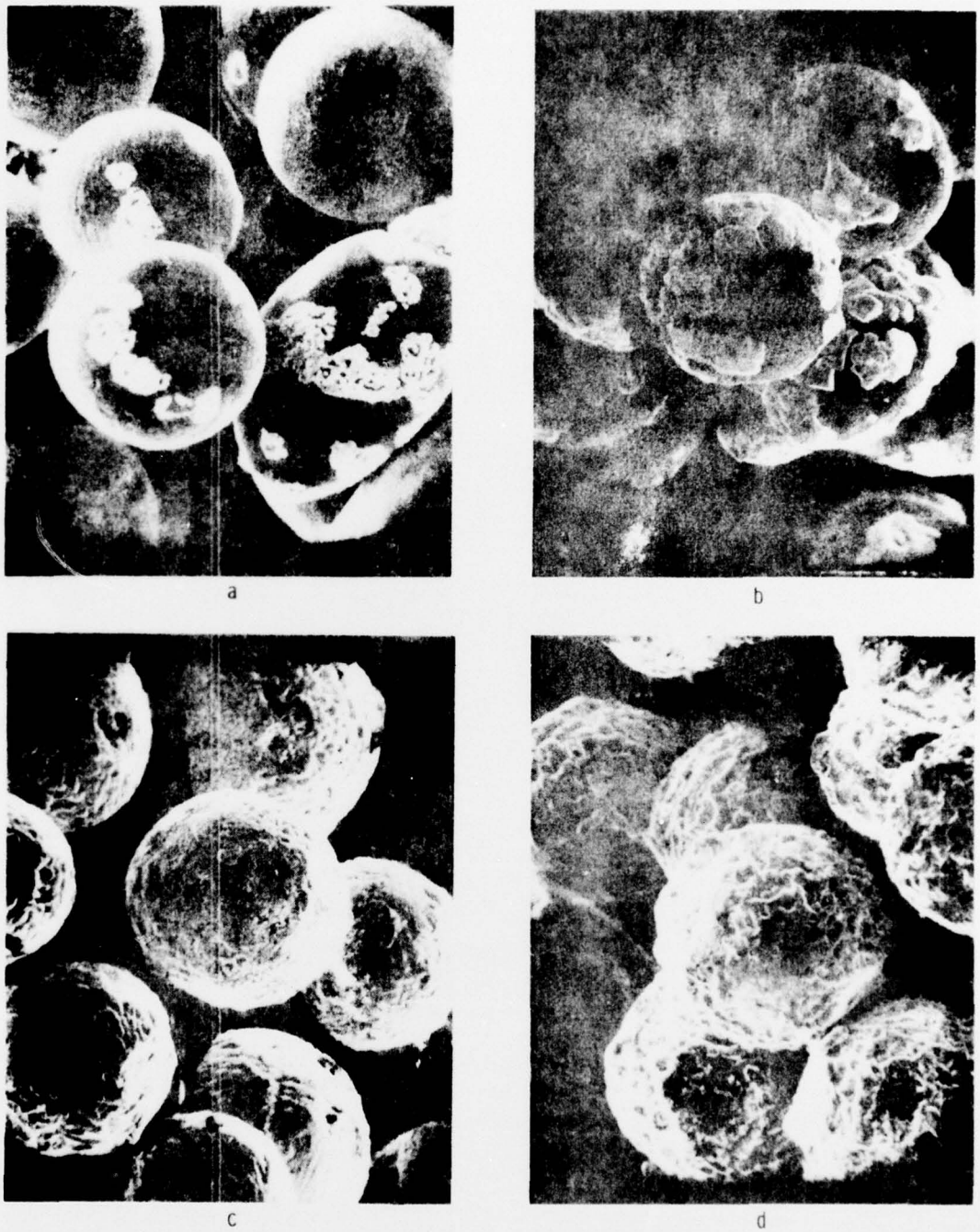

Figure 4. Evolution of surface morphology. Photographs taken at: a - 1.0 minute, b - 2.0 minutes, c - 5.5 minutes, d - 7.5 minutes (cf. Fig. 3 for j(x)).

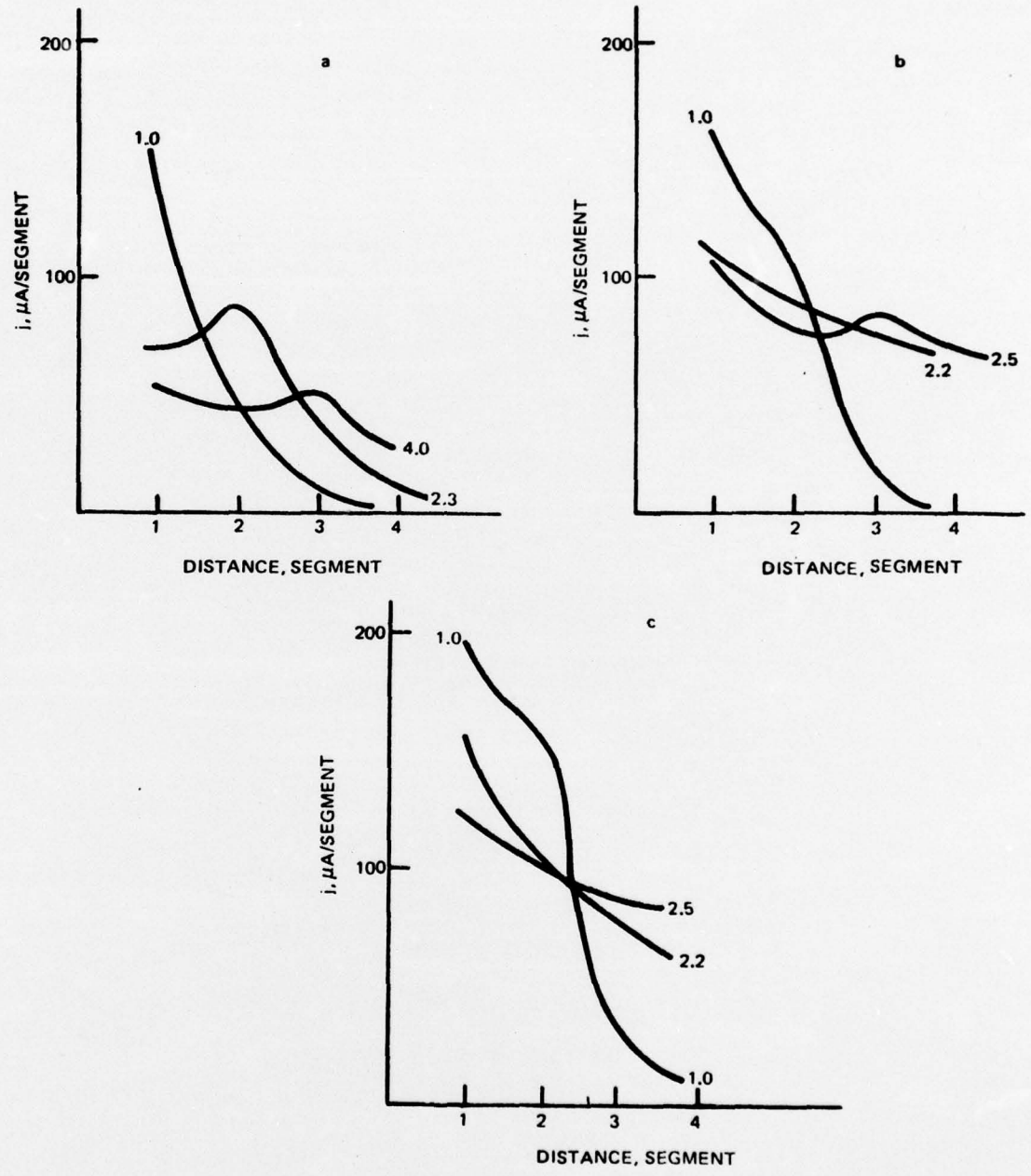

Figure 5. Effect of charging current.
a - 200 μA. b - 300 μA. c - 400 μA.
(Profiles plotted for times indicated.)

ENCL 2 TO LMSC D506557

TECHNICAL REPORT DISTRIBUTION LIST

	No. Copies
Office of Naval Research Arlington, Virginia 22217 Attn: Code 472	2
Office of Naval Research Arlington, Virginia 22217 Attn: Code 102IP	6
ONR Branch Office 536 S. Clark Street Chicago, Illinois 60605 Attn: Dr. George Sandoz	1
ONR Branch Office 715 Broadway New York, New York 10003 Attn: Scientific Dept.	1
ONR Branch Office 1030 East Green Street Pasadena, California 91106 Attn: Dr. R. J. Marcus	1
ONR Branch Office 760 Market Street, Rm. 447 San Francisco, California 94102 Attn: Dr. P. A. Miller	1
ONR Branch Office 495 Summer Street Boston, Massachusetts 02210 Attn: Dr. L. H. Peebles	1
Director, Naval Research Laboratory Washington, D.C. 20390 Attn: Library, Code 2029 (ONRL) Technical Info. Div. Code 6100, 6170	6 1 1
The Asst. Secretary of the Navy (R&D) Department of the Navy Room 4E736, Pentagon Washington, D.C. 20350	1
Commander, Naval Air Systems Command Department of the Navy Washington, D.C. 20360 Attn: Code 310C (H. Rosenwasser)	1

	No. Copi
Defense Documentation Center Building 5, Cameron Station Alexandria, Virginia 22314	12
U.S. Army Research Office P.O. Box 12211 Research Triangle Park, North Carolina 27709 Attn: CRD-AA-IP	
Commander Naval Undersea Research & Development Center San Diego, California 92132 Attn: Technical Library, Code 133	1
Naval Weapons Center China Lake, California 93555 Attn: Head, Chemistry Division	1
Naval Civil Engineering Laboratory Port Hueneme, California 93041 Attn: Mr. W. S. Haynes	1
Professor O. Heinz Department of Physics & Chemistry Naval Postgraduate School Monterey, California 93940	
Dr. A. L. Slafkosky Scientific Advisor Commandant of the Marine Corps (Code RD-1) Washington, D.C. 20380	1

ENCL 2 TO LMSC D506557

TECHNICAL REPORT DISTRIBUTION LIST

	No. Copies
Dr. Paul Delahay New York University Department of Chemistry New York, New York 10003	1
Dr. R. A. Osteryoung Colorado State University Department of Chemistry Fort Collins, Colorado 80521	1
Dr. E. Yeager Case Western Reserve University Department of Chemistry Cleveland, Ohio 41106	1
Dr. D. N. Bennion University of California Energy Kinetics Department Los Angeles, California 90024	1
Dr. J. W. Kauffman Northwestern University Department of Materials Science Evanston, Illinois 60201	1
Dr. R. A. Marcus University of Illinois Department of Chemistry Urbana, Illinois 61801	1
Dr. M. Eisenberg Electrochimica Corporation 2485 Charleston Road Mountain View, California 94040	1
Dr. J. J. Auborn GTE Laboratories, Inc. 40 Sylvan Road Waltham, Massachusetts 02154	1
Dr. Adam Heller Bell Telephone Laboratories Murray Hill, New Jersey	1
~~Dr. T. Katan~~ ~~Lockheed Missiles & Space Co., Inc.~~ ~~P.O. Box 504~~ ~~Sunnyvale, California 94088~~	1
Dr. R. A. Huggins Stanford University Department of Materials Science & Engineering Stanford, California 94305	1
Dr. Joseph Singer, Code 302-1 NASA-Lewis 21000 Brookpark Road Cleveland, Ohio 44135	1
Dr. B. Brummer EIC Incorporated Five Lee Street Cambridge, Massachusetts 02139	1
Library P. R. Mallory and Company, Inc. P. O. Box 706 Indianapolis, Indiana 46206	1
Dr. P. J. Hendra University of Southampton Department of Chemistry Southampton S09 5NH United Kingdom	
Dr. Sam Perone Purdue University Department of Chemistry West Lafayette, Indiana 47907	1
Dr. Royce W. Murray University of North Carolina Department of Chemistry Chapel Hill, North Carolina 27514	1
Dr. J. Proud GTE Laboratories Inc. Waltham Research Center 40 Sylvan Road Waltham, Massachusetts 02154	1
Mr. J. F. McCartney Naval Undersea Center Sensor and Information Technology Dept. San Diego, California 92132	1

TECHNICAL REPORT DISTRIBUTION LIST

	No. Copies
Dr. J. H. Ambrus The Electrochemistry Branch Materials Division, Research & Technology Dept. Naval Surface Weapons Center White Oak Laboratory Silver Spring, Maryland 20910	1
Dr. G. Goodman Globe-Union Inc. 5757 North Green Bay Avenue Milwaukee, Wisconsin 53201	1
Dr. J. Boechler Electrochimica Corporation Attention: Technical Library 2485 Charleston Road Mountain View, California 94040	1
Dr. D. L. Warburton The Electrochemistry Branch Materials Division, Research & Technology Dept. Naval Surface Weapons Center White Oak Laboratory Silver Spring, Maryland 20910	1
Dr. R.C. Chudacek McGraw-Edison Company Edison Battery Division Post Office Box 28 Bloomfield, New Jersey 07003	1